Nature of the induced ferroelectric phases in $TbMn_2O_5$

P. Tolédano
Laboratory of Complex Systems, 33 rue Saint-Leu, University of Picardie, 80000 Amiens, France

W. Schranz and G. Krexner
Faculty of Physics, University of Vienna, Boltzmanngasse 5, A-1090 Vienna, Austria

(Dated: January 22, 2010)

The magnetostructural transitions and magnetoelectric effects reported in $TbMn_2O_5$ are described theoretically and shown to correspond to two essentially different mechanisms for the induced ferroelectricity. The incommensurate and commensurate phases observed between 38 K and 24 K exhibit a hybrid pseudo-proper ferroelectric nature resulting from an effective bilinear coupling of the polarization with the antiferromagnetic order-parameter. This explains the high sensitivity of the dielectric properties of the material under applied magnetic field. Below 24 K the incommensurate phase shows a standard improper ferroelectric character induced by the coupling of two distinct magnetic order-parameters. The complex dielectric behavior observed in the material reflects the crossover from one to the other transition regime. The temperature dependences of the pertinent physical quantities are worked out and previous theoretical models are discussed.

PACS numbers: 61.50.Ah, 77.80.-e, 75.80.+q

I. INTRODUCTION

It was recently observed[1,2] that an electric polarization can emerge at a magnetic transition if the magnetic spins order in non-collinear spiral structures. This new type of magnetostructural transition was reported in various classes of multiferroic materials[3–6], such as the rare-earth manganites $RMnO_3$[7] and RMn_2O_5[8,9], $Ni_3V_2O_8$[10], $MnWO_4$[11], $CoCr_2$[12] or Cr_2BeO_4[13]. In these compounds the correlation between spins and electric dipoles gives rise to remarkable magnetoelectric effects, indicating a strong sensitivity to an applied magnetic field, such as reversals or flops of the polarization, and a strong enhancement of the dielectric permittivity. In the aforementioned materials the ferroelectric phases appear below an intermediate non-polar magnetic phase, i.e. the breaking of inversion symmetry, which allows emergence of ferroelectric properties, does not occur simultaneously with the breaking of time reversal symmetry.

Theoretical arguments have been raised[14–18] to justify the observation of magnetoelectric effects in spiral magnets. However, a comprehensive theoretical description of the experimental results disclosed in multiferroic materials could not be achieved because the actual symmetries of the primary (magnetic) and secondary (structural) order-parameters have not been related organically to the thermodynamic functions which provide the relevant phase diagrams. Here, we give a unifying theoretical description of the magnetostructural transitions found in the manganite $TbMn_2O_5$[8,9,19,20] in the framework of the Landau theory of magnetic phase transitions[21–23]. It reveals that the transitions observed in this compound at 38 K and 24 K correspond to essentially different mechanisms for the induced ferroelectricity: The 38 K transition involves an *effective bilinear* coupling of the polarization with a *single* magnetic order-parameter. It results in a *pseudo-proper* ferroelectric nature for the phases stable between 38 K and 24 K. By contrast, the 24 K transition exhibits an *improper* ferroelectric behavior corresponding to a linear-quadratic coupling of the polarization with *two distinct* magnetic order-parameters. The crossover from one to the other transition mechanism provides an interpretation of the dielectric behavior observed in absence or presence of an applied magnetic field[8,9].

On cooling below the paramagnetic Pbam1' (P) structure, $TbMn_2O_5$ undergoes five phase transitions[8,9] taking place successively at $T_1 = 43$ K, $T_2 = 38$ K, $T_3 = 33$ K, $T_4 = 24$ K and $T_5 = 10$ K, the corresponding phases being denoted I to V. The paper is organized as follows: In Sec. II the P$\rightarrow$ I $\rightarrow$ II $\rightarrow$ III sequence of transitions giving rise at T_1, T_2 and T_3, to the incommensurate phases I and II, and commensurate phase III[8,9], is described theoretically. The remarkable magnetoelectric effects ocurring at the III$\rightarrow$ IV $\rightarrow$ V transitions, taking place at T_4 and T_5, are analyzed in Sec. III. In Sec. IV our results are summarized and compared to the results obtained in previous theoretical works on $TbMn_2O_5$[24–30]. Adaption of our description to other RMn_2O_5 compounds[31–36] is outlined.

II. THE P$\rightarrow$ I $\rightarrow$ II $\rightarrow$ III TRANSITIONS

The wave-vector associated with the incommensurate antiferromagnetic phase I and ferroelectric phase II is $\vec{k} = (1/2, 0, k_z)$, with k_z decreasing from about 0.30 to 0.25. It is associated with a 4-dimensional irreducible corepresentation (IC) of Pbam1', denoted G_1, whose generators are given in Table I. The complex amplitudes $S_1 = \rho_1 e^{i\theta_1}$, $S_1^* = \rho_1 e^{-i\theta_1}$, $S_2 = \rho_2 e^{i\theta_2}$, $S_2^* = \rho_2 e^{-i\theta_2}$ of the magnetic waves transforming according to G_1, form the symmetry-breaking order-parameter for the P$\rightarrow$ I $\rightarrow$ II transitions, giving rise to the invariants $\mathfrak{I}_1 = \rho_1^2 + \rho_2^2$, $\mathfrak{I}_2 = \rho_1^2\rho_2^2$, and $\mathfrak{I}_3 = \rho_1^2\rho_2^2 cos2\theta$, with $\theta = \theta_1 - \theta_2$.

Pbam1′		$(U_z \mid 000)$	$(\sigma_x \mid \frac{a}{2}\frac{b}{2}0)$	$(I \mid 000)$	T	$(E \mid a00)$	$(E \mid 00c)$
G_1	S_1 S_1^* S_2 S_2^*	$\begin{bmatrix}1\\1\\1\\1\end{bmatrix}$	$\begin{bmatrix} & & & i\\ & & -i & \\ & i & & \\ -i & & & \end{bmatrix}$	$\begin{bmatrix} & 1 & & \\ 1 & & & \\ & & & 1\\ & & 1 & \end{bmatrix}$	$\begin{bmatrix}-1\\-1\\-1\\-1\end{bmatrix}$	$\begin{bmatrix}-1\\-1\\-1\\-1\end{bmatrix}$	$\begin{bmatrix}e^{i\varepsilon}\\e^{-i\varepsilon}\\e^{i\varepsilon}\\e^{-i\varepsilon}\end{bmatrix}$
Ξ_1	η_1 η_1^* η_2 η_2^*	$\begin{bmatrix} & 1 & & \\ & & & 1\\ 1 & & & \\ & 1 & & \end{bmatrix}$	$\begin{bmatrix} & & e^{i\varepsilon'} & \\ & & & e^{-i\varepsilon'}\\ e^{-i\varepsilon'} & & & \\ & e^{i\varepsilon'} & & \end{bmatrix}$	X	X	$\begin{bmatrix}e^{i\varepsilon'}\\e^{-i\varepsilon'}\\e^{i\varepsilon'}\\e^{-i\varepsilon'}\end{bmatrix}$	X
Ξ_2	ς_1 ς_1^* ς_2 ς_2^*	X	$\begin{bmatrix} & & -e^{i\varepsilon'} & \\ & & & -e^{-i\varepsilon'}\\ -e^{-i\varepsilon'} & & & \\ & -e^{i\varepsilon'} & & \end{bmatrix}$	X	X	X	X

Tab. I: Generators of the IC's G_1, Ξ_1 and Ξ_2. Diagonal 4×4 matrices are represented by columns. A cross ($\times$) indicates that the matrix is the same as in the upper row. $\epsilon = k_z c$ except in the commensurate phase III where $\epsilon = \frac{\pi}{2}$. $\epsilon' = k_x \frac{a}{2}$. G_1 is deduced from the irreducible representation (IR) of the group G_k=mm2, denoted $\hat{\tau}_1(k_{16})$ in Kovalev's tables[38]. Ξ_1 and Ξ_2 are deduced from the IR's ($\hat{\tau}_1(k_3)$ and $\hat{\tau}_2(k_3)$) of $G_k = m_y$.

Therefore the homogeneous part of the free-energy density reads:

$$\Phi_1(\rho_1,\rho_2,\theta) = \qquad (1)$$
$$a_1\Im_1 + a_2\Im_1^2 + b_1\Im_2 + b_2\Im_2^2 + c_1\Im_3 + c_2\Im_3^2 + d\Im_1\Im_3 + ...$$

An eighth degree expansion is required in order to account for the full set of stable phases resulting from the minimization of Φ_1 and for disclosing the magnetoelectric properties observed in $TbMn_2O_5$. It stems from the following rule demonstrated in Ref. 37: If n is the highest degree of the basic order-parameter invariants (here n=4 for the $\Im_2$ and $\Im_3$ invariants), the free energy has to be truncated at not less than the degree 2n (here 2n=8) for ensuring the stability of all phases involved in the phase diagram. However, one can neglect most of the non-independent invariants of degrees lower or equal to eight (as for example $\Im_1^3$, $\Im_1^4$, $\Im_1\Im_2$ or $\Im_2\Im_3$) which can be shown to have no influence on the stability of the phases, but only modify secondary features of the phase diagram, as for example the shape of the transition lines separating the stable phases. In contrast the invariant $\Im_1\Im_3$ has to be taken into account for stabilizing "asymmetric" phases with $\rho_1 \neq \rho_2$. Note that the fourth-degree invariants $\rho_1^2\rho_2^2$ and $\rho_1^2\rho_2^2 cos2\theta$ express at a phenomenological level the exchange striction interactions and anisotropic exchange forces, respectively. Minimizing Φ_1 with respect to θ yields the following equation of state:

$$\rho_1^2\rho_2^2 sin2\theta\left[c_1 + d_1(\rho_1^2+\rho_2^2) + 2c_2\rho_1^2\rho_2^2 cos2\theta\right] = 0 \qquad (2)$$

Eq.(2) and the equations minimizing Φ_1 with respect to ρ_1, ρ_2 show that *seven* phases, labeled 1-7, can be stabilized below the P phase for different equilibrium values of ρ_1, ρ_2 and θ. Fig. 1 summarizes the equilibrium properties of each phase and their magnetic point-group symmetries. One can verify that the phases denoted 2,4,6 and 7 display a ferroelectric polarization along y and that all phases correspond to an antiferromagnetic ordering except phases 5 and 7 which show a non-zero magnetization along x. The respective location of the phases is indicated in the theoretical phase diagrams shown in Fig. 2, in the space (a_1, b_1, c_1) (Fig. 2(a)) and plane (b_1, c_1) (Fig. 2(b)) of the phenomenological coefficients, and in the orbit space $(\Im_1, \Im_2, \Im_3)$ (Fig. 2(c)). It allows to determine the possible sequences of phases separated by second-order transitions as P→1→6→7 or P→3→4→7. Dielectric and magnetic properties of the phases are deduced from the coupling of the order-parameter with the polarization ($\vec{P}$)- and magnetization ($\vec{M}$)- components, which are $\Im_4 = \rho_1\rho_2 P_y \sin\theta$, $\Im_5 = (\rho_1^2 - \rho_2^2)M_xM_y$ and $\Im_6 = \rho_1\rho_2 M_xM_z\cos\theta$.

The preceding results allow a consistent interpretation of the P→ I → II sequence of phases reported in $TbMn_2O_5$. Phase I observed between T_1 and T_2, corresponds to phase 1 ($\rho_1 \neq 0$, $\rho_2 = 0$) in Fig. 1. It displays the m'm'm symmetry with antiferromagnetic order in the (x,y) plane ($\Im_5 = \rho_1^2 M_xM_y$), a doubling of the lattice parameter a and an incommensurate modulation along c, expressed by the Lifshitz invariant $\rho_1^2\frac{\partial\theta_1}{\partial z}$. Figs. 1 and 2 show that

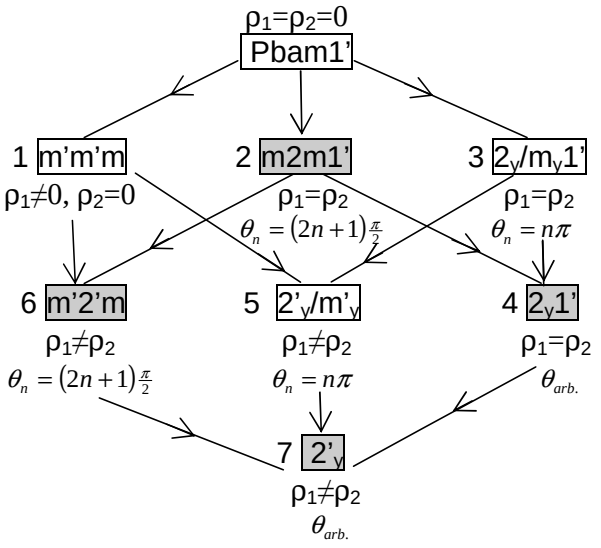

Fig. 1: Connections between the magnetic point-groups of phases 1-7 induced by the IC G_1 of Pbam 1', and equilibrium conditions fulfilled by the order-parameter in each phase. Gray rectangles indicate ferroelectric phases. $\theta_{arb.}$ stands for arbitrary.

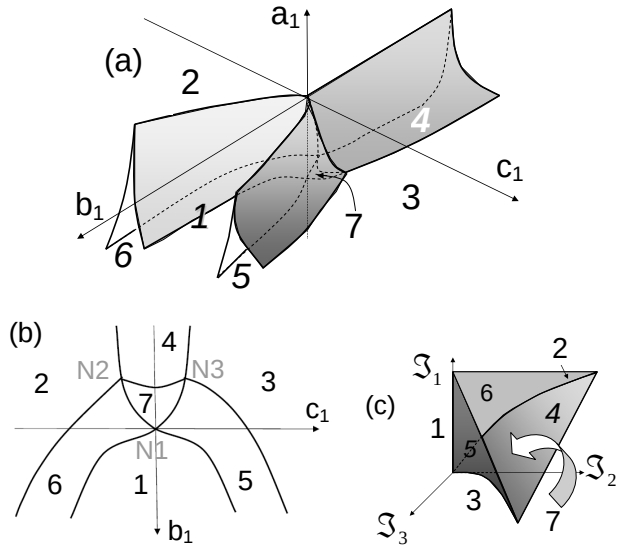

Fig. 2: Phase diagrams deduced from the minimization of the free-energy Φ_1 given by Eq. (1) in: (a) the (a_1, b_1, c_1) space, (b) the (b_1, c_1) plane for $a_1 < 0$, and (c) the orbit space ($\mathfrak{I}_1$, $\mathfrak{I}_2$,$\mathfrak{I}_3$). In (a) the phases are separated by second-order transition surfaces, which become curves in (b). Phases 1, 2 and 3 can be reached directly from the P-phase across the second-order plane $a_1 = 0$. In (b) N1, N2 and N3 are four-phase points, which become curves in (a). In (c) phases (1, 2, 3) and (4, 5, 6) correspond, respectively, to curves and surfaces. Phase 7 coincides with the volume limited by the surfaces (4, 5, 6).

a continuous transition can occur from phase 1 to the ferroelectric phase 6 ($\rho_1 \neq \rho_2$, $\theta = (2n+1)\frac{\pi}{2}$), which exhibits a spontaneous polarization along y, and a magnetic symmetry m'2'm preserving an antiferromagnetic order in the (x,y) plane ($\mathfrak{I}_5 \neq 0$). Identifying phase 6 with phase II of $TbMn_2O_5$ allows a straightforward interpretation of the dielectric behavior observed at the I $\rightarrow$ II transition. From the dielectric free-energy density $\Phi_1^D = \delta_1\rho_1\rho_2 P_y \sin\theta + \frac{P_y^2}{2\epsilon_{yy}^0}$, one gets the equilibrium value of P_y in phase 6

$$P_y^e = \pm\delta_1\epsilon_{yy}^0\rho_1\rho_2 \tag{3}$$

The (S_1, S_1^*) components related to ρ_1 have been already activated in phase 1, and *are frozen in phase 6* , which is induced by the sole symmetry breaking mechanism related to ρ_2. Therefore, Eq. (3) reflects an *effective bilinear coupling* of P_y with ρ_2, giving rise to a *proper ferroelectric* critical behavior at the transition between phases 1 and 6. This situation is reminiscent of *pseudo-proper ferroelectric transitions*[23] where the spontaneous polarization has the same symmetry as the transition order-parameter, to which it couples bilinearly, but results from an induced mechanism. In Phase II of $TbMn_2O_5$, P_y and ρ_2 are related by a *pseudo-proper-like* coupling since they display different symmetries. Therefore, at the I $\rightarrow$ II transition, P_y varies critically as ρ_2, i.e. $P_y \propto (T_2 - T)^{1/2}$, whereas the dielectric permittivity ϵ_{yy} exhibits a Curie-Weiss-like divergence $\epsilon_{yy} \propto \mid T - T_2 \mid^{-1}$. Figs. 3(a) and 3(b) show the excellent fit of the experimental curves reported by Hur et al.[8] with the preceding power-laws. The *induced* character of P_y appears only from its magnitude (40 nC cm^{-2})[8,9], which is two orders smaller than in proper ferroelectrics. Note that a conventional trilinear (improper) coupling between P_y and the magnetic order-parameters ρ_1 and ρ_2 would lead to an *upward step* of ϵ_{yy} and to a *linear* dependence of $P_y \propto (T_2 - T)$.

At $T_3 = 33$ K the wave vector locks into the commensurate value $\vec{k} = (\frac{1}{2}, 0, \frac{1}{4})$. Table I shows that the symmetry of the (S_1, S_1^*, S_2, S_2^*) order-parameter remains unchanged at the lock-in transition, with the exception of the matrix of the translation $(E|00c)$, allowing formation of the additional (Umklapp-) invariant $\rho_1^4 cos4\theta_1 + \rho_2^4 cos4\theta_2$, which triggers the onset of the commensurate phase. Therefore, Fig. 1 includes the lock-in commensurate phase III, which involves a fourfold multiplication of the c-lattice parameter, instead of an incommensurate modulation along z. The onset of phase III is reflected by a slight change in the slope of the polarization, with no noticeable anomaly of the dielectric permittivity. It suggests that the magnetic symmetry m'2'm of phase II remains unchanged in phase III.

III. THE III→IV→V TRANSITIONS

The wave-vector $\vec{k} = (k_x, 0, k_z) \approx (0.48, 0, 0.32)$ associated with the III→IV commensurate-incommensurate

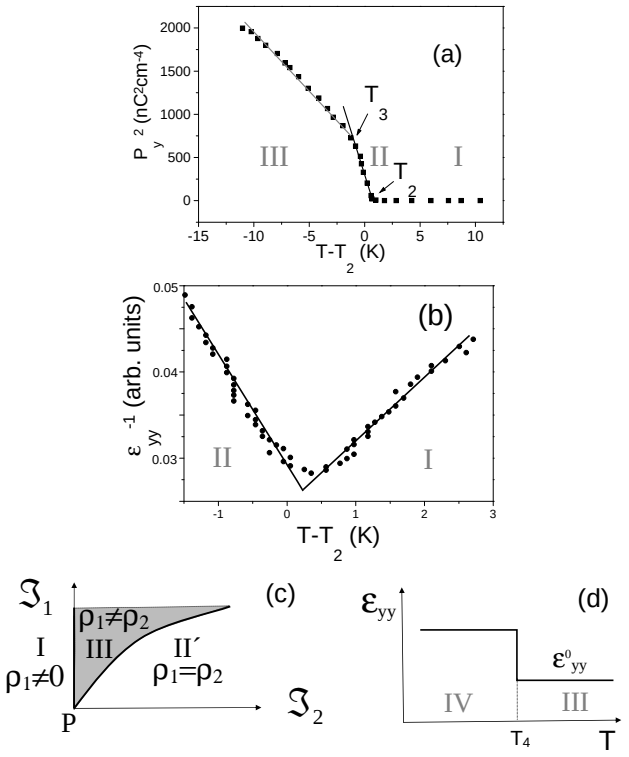

Fig. 3: (a) Least squares fits for the squared polarization $P_y^2 \propto (T_2 - T)$ and (b) the inverse dielectric permittivity $\epsilon_{yy}^{-1} \propto |(T_2 - T)|$ reported by Hur et al[8] . (c) Phase diagram associated with Ξ_1 in the orbit space $(\mathfrak{I}_1, \mathfrak{I}_2)$. The structural point-groups are $2_y/m_y$ (phase I), $2_z/m_z$ (phase II) and $\overline{1}$ (phase III). (d) Dielectric permittivity $\epsilon_{yy}(T)$ at the III $\rightarrow$ IV transition.

transition occurring at T_4, corresponds to two 4-dimensional IC´s of Pbam1', denoted Ξ_1 and Ξ_2, whose generators are given in Table I. The four-component order-parameters spanning the two IC´s can be written $(\eta_1 = \rho_1 e^{i\phi_1}, \eta_1^* = \rho_1 e^{-i\phi_1}, \eta_2 = \rho_2 e^{i\phi_2}, \eta_2^* = \rho_2 e^{-i\phi_2})$ for Ξ_1 and $(\varsigma_1 = \rho_3 e^{i\phi_3}, \varsigma_1^* = \rho_3 e^{-i\phi_3}, \varsigma_2 = \rho_4 e^{i\phi_4}, \varsigma_2^* = \rho_4 e^{-i\phi_4})$ for Ξ_2. It yields the following independent order-parameter invariants: $(\mathfrak{I}_1 = \rho_1^2 + \rho_2^2, \mathfrak{I}_2 = \rho_1^2\rho_2^2)$ for Ξ_1 , and $(\mathfrak{I}_3 = \rho_3^2 + \rho_4^2, \mathfrak{I}_4 = \rho_3^2\rho_4^2)$ for Ξ_2.

Minimization of the free energy associated with Ξ_1 yields three possible stable states, shown in the $(\mathfrak{I}_1, \mathfrak{I}_2)$ phase diagram of Fig. 3(c), which display the *non-polar* structural symmetries $2_y/m_y(\rho_1 \neq 0, \rho_2 = 0), 2_z/m_z(\rho_1 = \rho_2)$ and $\bar{1}(\rho_1 \neq \rho_2 \neq 0)$. The same non-polar symmetries are induced by Ξ_2. Therefore, ferroelectric phases IV and V may only result from a *coupling* of the (η_i) and (ς_i) order-parameters associated with $\Xi_1 + \Xi_2$, consistent with the observation by Koo et al.[20] of a multiple magnetic ordering in phase IV. Taking into account the coupling invariant $\mathfrak{I}_5 = \rho_1^2\rho_3^2 cos2\Psi_1 + \rho_2^2\rho_4^2 cos2\Psi_2$, with $\Psi_1 = \Phi_1 - \Phi_3$ and $\Psi_2 = \Phi_2 - \Phi_4$, the free-energy associated with $\Xi_1 + \Xi_2$ reads:

$$\Phi_2(\rho_i, \Psi_i) = \sum_{i=1}^{5} (\alpha_i \mathfrak{I}_i + \beta_i \mathfrak{I}_i^2) \qquad (4)$$

Minimization of Φ_2 shows that not less than 15 distinct phases can be stabilized for different equilibrium values of ρ_i and Ψ_i. 6 of these phases display a ferroelectric polarization component P_y, resulting from the mixed coupling invariant: $\mathfrak{I}_6 = P_y(\rho_1\rho_3 sin\Psi_1 + \rho_2\rho_4 sin\Psi_2)$. For $\rho_1 = \rho_2$, $\rho_3 = \rho_4$, $\Psi_1 = (2n+1)\frac{\pi}{2}$ or (and) $\Psi_2 = n\frac{\pi}{2}$ the phases have the structural symmetry m2m. For $\rho_1 \neq 0, \rho_3 \neq 0, \rho_2 = \rho_4 = 0$ or $\rho_1 = \rho_3 = 0, \rho_2 \neq 0, \rho_4 \neq 0$ or $\rho_1 \neq \rho_2$, $\rho_3 \neq \rho_4$ with Ψ_1 or $\Psi_2 = (2n+1)\frac{\pi}{2}$ and Ψ_1 or Ψ_2 arbitrary, or Ψ_1 and Ψ_2 arbitrary, the structural symmetry is lowered to 2_y. The magnetic order in the different phases is expressed by the coupling invariants $\mathfrak{I}_7 = M_x M_y(\rho_1\rho_3 cos\Psi_1 + \rho_2\rho_4 cos\Psi_2)$ and $\mathfrak{I}_8 = M_y M_z(\rho_1\rho_3 cos\Psi_1 - \rho_2\rho_4 cos\Psi_2)$.

The experimental results reported for the magnetic structure of phase IV of $TbMn_2O_5$[20] are consistent with a structural symmetry m2m. One can assume, without loss of generality, that the corresponding equilibrium values of the order-parameters in phase IV are $\rho_1 = \rho_2$, $\rho_3 = \rho_4$, $\Psi_1 = (2n+1)\frac{\pi}{2}$, $\Psi_2 = n\pi$. Therefore the dielectric contribution to the free-energy at the III$\rightarrow$IV transition is: $\Phi_2^D = \pm\delta_2\rho_1\rho_3 P_y + \frac{P_y^2}{2\epsilon_{yy}^0}$. It yields

$$P_y^e = \pm\delta_2 \epsilon_{yy}^0 \rho_1 \rho_3 \qquad (5)$$

Since both order-parameters ρ_1 *and* ρ_3 contribute to the symmetry-breaking mechanism at T_4, they both vary as $\propto (T_4 - T)^{1/2}$ for $T \leq T_4$. Therefore P_y varies linearly as $(T_4 - T)$, which expresses a typical improper ferroelectric behaviour for the III$\rightarrow$IV transition. The dielectric permittivity is given by $\epsilon_{yy} = \epsilon_{yy}^0(1 - \delta_2 \frac{\partial \rho_1 \rho_3}{\partial E_y})$, where E_y is the applied electric field. It yields $(\epsilon_{yy} = \epsilon_{yy}^0)$ for $T > T_4$, and is approximated by $\epsilon_{yy} \approx \frac{\epsilon_{yy}^0 y}{1 - \delta_2^2 \epsilon_{yy}^0 f(\beta_i, \alpha_5)}$ for $T < T_4$, where $f(\beta_i, \alpha_5)$ represents a combination of phenomenological coefficients of Φ_2 with $0 < f(\beta_i, \alpha_5) < 1$. Accordingly, $\epsilon_{yy}(T)$ undergoes an *upward step* at T_4 (Fig. 3 (d)), as observed experimentally[8,9]. Note that the change in the order-parameter symmetry imposes a first-order character to the III$\rightarrow$IV transition, consistent with the lattice anomalies observed at 24 K[9].

The preceding description allows a straightforward explanation of the observed decrease[8] of the equilibrium polarization P_y^e at zero magnetic field which is starting at about 26 K. Below T_4, P_y^e is the sum of two distinct contributions given by Eqs. (3) and (5).

$$P_y^e = \pm\epsilon_{yy}^0[\delta_1\rho_1(T_2 - T)^{1/2} + \delta_2(T_4 - T)] \qquad (6)$$

where $\rho_1 \propto (T_1 - T_2)^{1/2}$. Assuming $\delta_1 > 0$ and $\delta_2 < 0$, one can verify that P_y^e decreases for $T \leq T_{max} = T_2 - \frac{\delta_1^2(T_1 - T_2)}{4\delta_2^2}$. This explanation confirms the conjec-

ture by Hur, et al.[8] that the total polarization is composed by positive and negative components, which appear at T_2 and T_4, respectively. The opposite signs of P_y^e in Eq.(6) correspond to the opposite ferroelectric domains disclosed by the preceding authors under opposite electric fields. The strong increase of P_y^e observed below T_5 reflects the positive contribution of phase V to the total polarization. The absence of dielectric anomaly at T_5 suggests that the m2m symmetry of phase IV remains unchanged in phase V with an eventual change in the respective values of Ψ_1 or (and) Ψ_2.

It remains to understand why the decrease of P_y is enhanced by application of a magnetic field H_x, leading to a change in sign of P_y above a threshold field H_x^c[8,9]. This can be explained by considering the magnetic and magnetoelectric contributions to the free-energy under H_x field in phase IV: $\Phi_2^M = \mu_0 \frac{M_x^2}{2} - H_x M_x$ and $\Phi_2^{ME} = \nu \rho_1 \rho_3 P_y M_x^2$. It yields for the field dependent spontaneous polarization in phase IV:

$$P_y^{IV}(H_x) = \pm \epsilon_{yy}^0 \rho_1 \rho_3 \Big(\delta_2 + \nu \mu_0^{-1} H_x^2 \Big) \qquad (7)$$

For $\nu < 0$ the application of an H_x field enhances the negative contribution P_y^{IV} to the temperature dependence of the total polarization leading to:

$$P_y^e(T, H_x) = \pm \epsilon_{yy}^0 \Big[\delta_1 (T_1 - T_2)^{1/2} (T_2 - T)^{1/2} + (\delta_2 + \nu \mu_0^{-1} H_x^2 (T_4 - T) \Big] \qquad (8)$$

Accordingly $P_y^e(T, H_x)$ changes sign for the temperature dependent threshold field:

$$H_x^c(T)^2 = \frac{\delta_1 \mu_0 (T_1 - T_2)^{1/2} (T_2 - T)^{1/2}}{|\delta_2 \mu_0 + \nu| (T_4 - T)} \qquad (9)$$

From Eqs. (8) and (9) one can verify that with increasing applied field, $P_y^e(T, H_x)$ decreases more sharply and changes sign at higher temperature (Fig.4), as was actually observed by Hur et al.[8].

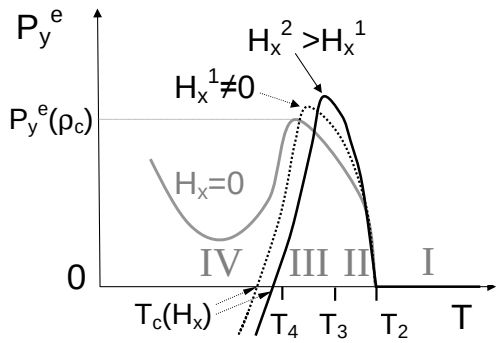

Fig. 4: Temperature dependence of $P_y^e(T, H_x)$ given by Eq. (8), for $\delta_1 > 0$, $\delta_2 < 0$ $\nu < 0$. With increasing field $P_y^e(T, H_x)$ decreases more sharply and is shifted to higher temperature. The change in sign of $P_y^e(T, H_x)$ occurs at a field-dependent critical temperature $T_c(H_x)$.

IV. SUMMARY AND DISCUSSION

In summary, it has been shown that two distinct symmetry breaking ordering parameters are involved in the sequence of five magnetic phases found in $TbMn_2O_5$ below:

1) a single four-component order-parameter is associated with the P→I→II→III transitions. Two among the components (S_1, S_1^*) give rise at T_1 to the antiferromagnetic phase I, whereas the two others (S_2, S_2^*) are activated at T_2 , at the onset of the ferroelectric phase II, (S_1, S_1^*) being frozen at the I II transition. It results in a hybrid pseudo-proper ferroelectric behavior for this transition, which displays critical dielectric anomalies typical of proper ferroelectric transitions, although the magnitude of the induced polarization in phase II is of the order found in improper ferroelectrics. At the II→III transition the translational symmetry along z becomes commensurate, modifying in a minor way the ferroelectric properties of the material. The theoretical phase diagram showing the location of the phases stabilized in $TbMn_2O_5$, as well as the other five phases induced by the (S_i, S_i^*) order-parameter, has been worked-out, and the magnetic point-groups of the different phases have been given.

2) At the commensurate-incommensurate III→IV transition the (S_i, S_i^*) order-parameter splits into two distinct four-component order-parameters (η_i) and (ς_i), which couple for inducing the ferroelectric phases IV and V. The III→IV transition shows a standard improper ferroelectric behavior. The absence of noticeable anomaly for the dielectric permittivity at the IV→V transition suggests that the structural symmetry of phase IV remains unchanged in phase V. However, the spontaneous polarization in phase V contributes positively to the observed total polarization P_y^e, whereas phase IV exhibits a negative contribution to P_y^e. Opposite signs of the spontaneous electric polarizations in phases IV and V provide a consistent interpretation of the non-monotonous temperature dependence of $P_y^e(T)$ across the II→III→IV→V sequence of induced ferroelectric transitions. Application of an H_x magnetic field modifies the preceding behavior, via the magnetoelectric coupling between P_y and the induced magnetization M_x, which contributes negatively to the total polarization, explaining the observed change of sign of $P_y^e(T, H_x)$.

A number of previous studies[24–30] proposed a theoretical description of the dielectric and magnetoelectric properties of $TbMn_2O_5$. However, none of these studies took fully into account the order-parameter symmetries associated with the different phases. Therefore, the relevant free-energies, expanded to the necessary degrees, and the related coupling terms, could not be disclosed,

and the proper phase diagrams could not be derived. As a consequence, a consistent interpretation of the dielectric behavior at zero magnetic field, or under applied H_x field, could not be given explicitly. In contrast to our phenomenological description, based on the symmetry and thermodynamic considerations underlying the Landau theory of magnetic phase transitions[21–23], which is free from any microscopic model, the previous works, using different group-theoretical procedures, attempted to deduce the magnetoelectric properties of the material from its complex magnetic structures and related magnetic interactions. For example, Radaelli and Chapon limit their group-theoretical analysis to the irreducible corepresentations of the little group[24]. It does not allow determination of the transition free-energy and of the coupling relating the polarization to the magnetic order-parameter, which they deduce from microscopic coupling mechanisms[25]. The complex procedure proposed by Harris[26] for determining the transition order-parameter from the spin configuration of $TbMn_2O_5$ does not provide the relevant order-parameter symmetry, and is not related organically with the different effective free-energies used by Harris et al[27,28] for describing the ferroelectric transitions in this material. It leads to oversimplified phase diagrams and to a speculative interpretation of the observed dielectric and magnetoelectric properties. Besides, the critical wave vector assumed by Harris et al.[27] for phases I and II of $TbMn_2O_5$ corresponds actually to phases IV and V, which are not described by these authors. The Landau model used by Kadomtseva et al.[29] provides an insight into the exchange and relativistic magnetic contributions to the free-energy and induced polarization involved in RMn_2O_5 compounds. However, the dimensionality of the irreducible representation and order-parameter assumed in their model (2-dimension instead of two coupled 4-dimensional order-parameters required for $ErMn_2O_5$ and YMn_2O_5) and the fact that two successive and distinct order-parameters are needed for describing the full sequence of observed phases, do not allow these authors to describe consistently the observed dielectric properties and magnetoelectric effects. Along another line, the model proposed by Sushkov et al.[30] gives an interesting analysis of the underlying magnetic forces explaining the induced dielectric properties in the RMn_2O_5 family, but a detailed description of the observed phase sequences and magnetoelectric effects, that would require considering the actual order-parameter symmetries, is missing.

Similar sequences of ferroelectric phases are found in other RMn_2O_5 compounds[31–36] where $R = Bi, Y$ or a rare-earth heavier than Nd. In these compounds, with the exception of $BiMn_2O_5$, the first ferroelectric phase does not appear directly below the paramagnetic phase, but below an intermediate non-polar antiferromagnetic phase. Therefore the induced electric polarization results from the coupling of two distinct magnetic order-parameters, one of which having been already activated in the intermediate phase. As a consequence a pseudo-proper coupling is created, which gives rise to the typical critical behavior of a proper ferroelectric transition. In $TbMn_2O_5$ the first ferroelectric transition corresponds to $\vec{k} = (\frac{1}{2}, 0, k_z)$ and to a *single* 4-component order-parameter, the pseudo-proper coupling occurring between *distinct components* of the same order-parameter. A different situation is found in the other RMn_2O_5 compounds, in which the first transitions correspond to $\vec{k} = (k_x, 0, k_z)$[31–36], i.e. the pseudo-proper coupling occurs between *two distinct 4-component order-parameters* having the symmetries of the (η_i) and (ς_i) order-parameters, which are associated in the present work to the lower temperature transition sequence of $TbMn_2O_5$. The order-parameters involved in the RMn_2O_5 family correspond in most cases to the symmetries disclosed in the present work for $R = Tb$, i.e. to $\vec{k} = (\frac{1}{2}, 0, k_z)$, $(k_x, 0, k_z)$ and $(\frac{1}{2}, 0, \frac{1}{4})$. Two exceptions are presently known, which are:
1) The lower temperature phase of $DyMn_2O_5$[35] induced by bidimensional order-parameters corresponding to the wave-vector $(\frac{1}{2}, 0, 0)$, and
2) The single ferroelectric phase of $BiMn_2O_5$[36]induced by bidimensional IC's at $\vec{k} = (\frac{1}{2}, 0, \frac{1}{2})$.
Accordingly, despite the apparent variety of behaviors found for the dielectric properties and field effects a unifying theoretical framework can be proposed for the RMn_2O_5 manganites, which can be deduced from the description given in the present work, by interchanging the order-parameters in the observed transition sequences.

V. CONCLUSIONS

In conclusion, the order-parameter symmetries associated with the magnetostructural transitions observed in $TbMn_2O_5$ clarify the nature of the ferroelectric phases and permit a consistent description of the magnetoelectric effects observed in this material. In a more general way, our phenomenological approach illustrates the necessity of taking into account the actual order-parameter symmetries and phase diagrams associated with the phase sequences reported in multiferroic compounds. It can be used for analyzing the complex microscopic mechanisms and interactions involved in magnetostructural transitions, which have not been discussed in the present work.

Acknowledgments

Support by the Austrian FWF (P19284-N20) and by the University of Vienna within the IC Experimental Materials Science ("Bulk Nanostructured Materials") is gratefully acknowledged.

[1] T. Kimura, T. Goto, H. Shintani, K. Ishizaka, T. Arima and Y. Tokura, Nature **426**, 55 (2003).
[2] T. Kimura, Annu. Rev. Mater. Res. **37**, 386 (2007).
[3] M. Fiebig, J. Phys. D: Appl. Phys. **38**, R123 (2005).
[4] W. Eerenstein, N. D. Mathur, and J. F. Scott, Nature **442**, 759 (2006).
[5] R. Ramesh and N. A. Spaldin, Nature Materials **6**, 21 (2007).
[6] S. -W. Cheong and M. Mostovoy, Nature Materials **6**, 13 (2007).
[7] T. Goto, T. Kimura, G. Lawes, A. P. Ramirez and Y. Tokura, Phys. Rev. Lett. **92**, 257201 (2004).
[8] N. Hur, S. Park, P. A. Sharma, J. S. Ahn, S. Guha and S.-W. Cheong, Nature **429** 392 (2004).
[9] L. C. Chapon, G. R. Blake, M. J. Gutmann, S. Park, N. Hur, P. G. Radaelli and S.-W. Cheong, Phys. Rev. Lett. **93**, 177402 (2004).
[10] G. Lawes, A. B. Harris, T. Kimura, N. Rogado and R. J. Cava, Phys. Rev. Lett. **95**, 087205 (2005).
[11] K. Taniguchi, N. Abe, T. Takenobu, Y. Iwasa and T. Arima, Phys. Rev. Lett. **97**, 097203 (2006).
[12] K. Tomiyasu, J. Fukunaga and H. Suzuki, Phys. Rev. B **70**, 214434 (2004).
[13] R. E. Newnham, J. J. Kramer, W. A. Schulze and L. E. Cross, J. Appl. Phys. **49**, 6088 (1978).
[14] H. Katsura, N. Nagaosa and A. V. Balatsky, Phys. Rev. Lett. **95**, 057205 (2005).
[15] M. Mostovoy, Phys. Rev. Lett. **96**, 067601 (2006).
[16] I. A. Sergienko and R. Dagotto, Phys. Rev. B **73**, 094434 (2006).
[17] M. Kenzelmann, A. B. Harris, S. Jonas, C. Broholm, J. Schefer, S. B. Kim, C. L. Zhang, S.-W. Cheong, O. P. Vajk and J. W. Lynn, Phys. Rev. Lett, **95**, 087206 (2005).
[18] J. Hu, Phys. Rev. Lett, **100**, 077202 (2008).
[19] G. R. Blake, L. C. Chapon, P. G. Radaelli, S. Park, N. Hur, S.-W. Cheong and J. Rodriguez-Carvajal, Phys. Rev. B **71**, 214402 (2005).
[20] J. Koo, C. Song, S. Ji, J.-S. Lee, J. Park, T.-H. Jang, C.-H. Yang, J.-H. Park, Y. H. Jeong, K.-B. Lee, T.Y. Koo, Y. J. Park, J.-Y. Kim, D. Wermeille, A. I. Goldman, G. Srajer, S. Park and S.-W. Cheong, Phys. Rev. Lett. **99**, 197601 (2007).
[21] L. D. Landau, Zh. Eksper. Teor. Fiz. **7**, 627 (1937).
[22] I. E. Dzialoshinskii, Sov. Phys. JETP **19**, 960 (1964).
[23] J. C. Tolédano and P. Tolédano, *The Landau Theory of Phase Transitions*, World Scientific, Singapore (1987).
[24] P. G. Radaelli and L. C. Chapon, Phys. Rev. B **76**, 054428 (2007).
[25] P. G. Radaelli and L. C. Chapon, J. Phys: Condens. Matter **20**, 434213 (2008).
[26] A. B. Harris, Phys. Rev. B **76**, 054447 (2007).
[27] A. B. Harris, A. Aharony and O. Entin-Wohlman, J. Phys: Condens. Matter **20**, 434202 (2008).
[28] A. B. Harris, M. Kenzelmann, A. Aharony and O. Entin-Wohlman, Phys. Rev. B **78**, 014407 (2008).
[29] A. M. Kadomtseva, S. S. Krotov, Yu. F. Popov, G. P. Vorob´ev and M. M. Lukina, J. Exp. Theoret. Phys. **100**, 305 (2005).
[30] A. B. Sushkov, M. Mostovoy, R. Valdés Aguilar, S.-W. Cheong and H. D. Drew, J. Phys: Condens. Matter **20**, 434210 (2008).
[31] Y. Noda, H. Kimura, M. Fukunaga, S. Kobayashi, I. Kagomiya and K. Kohn, J. Phys: Condens. Matter **20**, 434206 (2008).
[32] L. C. Chapon, P. G. Radaelli, G. R. Blake, S. Park and S.-W. Cheong, Phys. Rev. Lett. **96**, 097601 (2006).
[33] Y. Bodenthin, U. Staub, M. Garcýa-Fernandez, M. Janoschek, J. Schlappa, E. I. Golovenchits, V. A. Sanina and S. G. Lushnikov, Phys. Rev. Lett. **100**, 027201 (2008).
[34] D. Higashiyama, S. Miyasaka and Y. Tokura, Phys. Rev. B **72**, 064421 (2005).
[35] N. Hur, S. Park, P. A. Sharma, S. Guha, and S-W. Cheong, Phys. Rev. Lett. **93** 107207 (2004).
[36] A. Munoz, J. A. Alonso, M. T. Casais, M. J. Martýnez-Lope, J. L. Martýnez and M. T. Fernandez-Dýaz, Phys. Rev. B **65**, 144423 (2002).
[37] P. Tolédano and V. Dmitriev, *Reconstructive Physe Transitions*, World Scientific, Singapore (1996).
[38] O. V. Kovalev, *The Irreducible Representation of Space Groups*, Gordon and Breach, New York (1965).

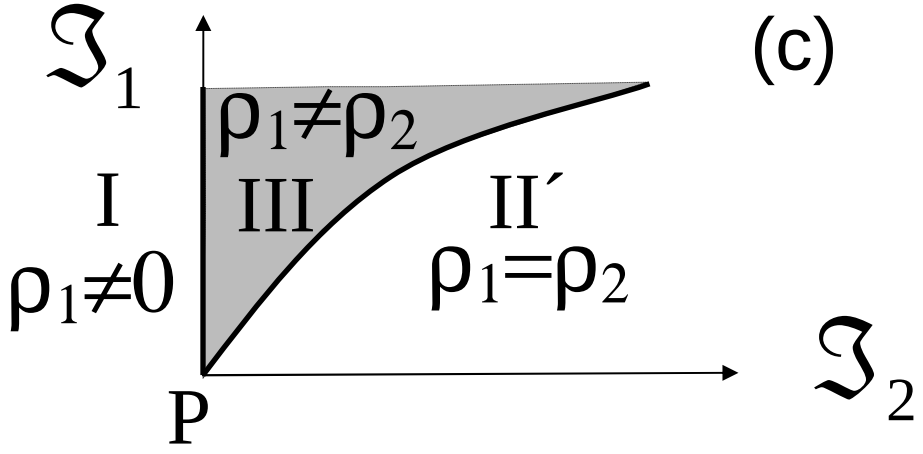
ℑ1
(c)
ρ1≠ρ2
I
ρ1≠0
III
II´
ρ1=ρ2
ℑ2
P